Efficient frequency conversion of incoherent fluorescent light

M. Katsuragawa, J. Q. Liang, Fam Le Kien,* and K. Hakuta
Department of Applied Physics and Chemistry, University of Electro-Communications, Chofu, Tokyo 182-8585, Japan
CREST, Japan Science and Technology Corporation (JST), Chofu, Tokyo 182-8585, Japan
(Received 19 April 2001; published 3 January 2002)

We demonstrate efficient replication of an incoherent fluorescent light with the 1770-cm^{-1} broad bandwidth into its Raman sidebands with frequency spacing of 4150 cm^{-1} in a thin hydrogen crystal. We achieve a high conversion efficiency of 22% per sideband using a sufficiently large Raman coherence prepared by two collinearly propagating ns laser fields.

DOI: 10.1103/PhysRevA.65.025801 PACS number(s): 42.50.Gy, 42.79.Nv, 42.50.Hz, 42.65.Ky

Optical parametric frequency conversion is an important method to obtain new light sources that can be used for various applications. To achieve an appreciable efficiency for the conversion process, one must overcome the phase mismatch originating from the refractive-index dispersion. Many methods have been developed so far to realize phase matching. Among them, a typical method is to make use of crystal birefringence for achieving phase matching. Although this method has been widely used for various purposes, it imposes a stringent restriction on the angular orientation of the crystal optical axis with respect to the polarization direction of the incident light [1]. Therefore, for lights with broad bandwidth, this method cannot work alone, and additional techniques are required. For example, in order to convert broadband lights, one has to carefully design the angular spread of the spectra to establish the so-called noncollinear phase matching [2,3].

Recently, it has been shown that a large coherence of a dipole-nonallowed transition in far-off-resonance Raman systems can lead to parametric Raman processes free from the stringent restriction on the angular orientations [4–6]. We have shown that a large Raman coherence established in solid hydrogen leads to parametric anti-Stokes Raman scattering without conventional phase matching [5]. More recently, we have demonstrated that a sufficiently large Raman coherence prepared by two coaxial single-mode lasers modulates an incident multimode laser radiation and efficiently replicates the broadband nature [300 cm^{-1} full width at half maximum (FWHM)] of the incident light into the higher- and lower-frequency sidebands with a frequency spacing of 4150 cm^{-1} [7].

In this paper we substantially develop the prepared-Raman-coherence technique [7] and extend it to an extreme case where the incident radiation is a temporally and spatially *incoherent fluorescent light*. We demonstrate efficient replication of an incoherent fluorescent light with the 1770-cm^{-1} broad bandwidth into its Raman sidebands with a frequency spacing of 4150 cm^{-1} in a thin hydrogen crystal. We achieve a high conversion efficiency of 22% per sideband using a sufficiently large Raman coherence prepared by two collinearly propagating ns laser fields. Unlike the multimode laser light used in the previous work [7], the fluorescent light used in our present paper is incoherent in space and time and has a huge bandwidth. As far as we know, this is the first report on the experimental realization of the parametric replication of *incoherent light* without conventional noncollinear phase matching.

Figure 1(a) shows the schematic of the generation of Raman sidebands E_q by beating a weak probe field E_0 with a prepared Raman-transition coherence ρ_{ab}. Under the far-off-resonance condition, the slowly varying envelope equation for E_q in the local time $\tau = t - z/c$ reads $\partial E_q/\partial z = i\beta_q(a_q E_q + d_{q-1}\rho_{ba}E_{q-1} + d_q\rho_{ab}E_{q+1})$, where a_q and d_q are the dispersion and coupling constants, respectively, and $\beta_q = N\hbar\omega_q/\epsilon_0 c$ [4,8]. Here ω_q is the carrier frequency of E_q and N is the number of molecules per volume. We restrict the discussion to the first Stokes and anti-Stokes sidebands. We assume that the absolute value and the phase shift per length of ρ_{ab} are constants, that is, $\rho_{ab}(z) = e^{i(\varphi_0 - \kappa_c z)}|\rho_{ab}(0)|$. When $\Delta\kappa_c = \kappa_c - (\beta_1 a_1 - \beta_{-1}a_{-1})/2$ is negligible, we find

$$E_{\pm 1}(z,\tau) = ig_{\pm 1}\frac{|\rho_{ab}|}{s}\sin(sz)e^{i\psi_{\pm 1}(z)}E_0^{(\mathrm{in})}(\tau),$$

$$s = \sqrt{g^2|\rho_{ab}|^2 + (\Delta\kappa/2)^2}, \tag{1}$$

where $g_1 = \beta_1 d_0$ and $g_{-1} = \beta_{-1}d_{-1}$ are the coupling parameters, $g = \sqrt{\beta_0(\beta_1 d_0^2 + \beta_{-1}d_{-1}^2)}$ is the effective coupling parameter, $\Delta\kappa = \kappa_0 - (\kappa_1 + \kappa_{-1})/2$ is a partial phase mismatch, $\kappa_q = \beta_q a_q$ are the single-mode phase shifts per length, $\psi_{\pm 1}(z) = (\kappa_{\pm 1} + \Delta\kappa/2)z \mp \varphi_0$ are the full phase shifts, and $E_0^{(\mathrm{in})}(\tau)$ is the input probe field. According to Eqs. (1), a

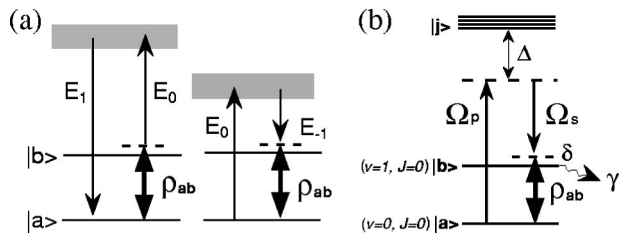

FIG. 1. (a) Collinear sideband generation ($E_0 \rightarrow E_{\pm 1}$) with a sufficiently large Raman coherence ρ_{ab}. (b) Preparation of the Raman coherence ρ_{ab} in solid parahydrogen.

*On leave from Department of Physics, University of Hanoi, Hanoi, Vietnam; also at Institute of Physics, National Center for Natural Sciences and Technology, Hanoi, Vietnam.

larger value of $|\rho_{ab}|/s$ leads to more efficient frequency conversion. The largest values of $|E_{\pm 1}|$ are achieved at the length $z=\pi/2s$. The condition

$$4g|\rho_{ab}| \gg \Delta K \equiv \max(2|\Delta\kappa|, |\Delta\kappa_c|) \tag{2}$$

is required for the maximum-gain length to be smaller than the coherence length $l_{\mathrm{coh}}=2\pi/\Delta K$. Under this condition, substantial frequency conversion occurs in the region of $z \cong \pi/2g|\rho_{ab}|$. Calculations show that, for the parameters of the experiment described below, condition (2) can be satisfied for the whole visible region. Condition (2) can be realized by two different methods. One is to reduce ΔK to near zero, a conventional method, known as phase matching. The other method is to generate a sufficiently large coherence ρ_{ab} against the inherent phase mismatch ΔK. With the use of this method, the frequency conversion process is free from the restriction on the phase relation between the probe and the generated fields. Therefore, this method can be used for lights with arbitrary spectral and statistical properties. The practical difficulty of this method lies in the realization of a substantial, long-living Raman coherence. We emphasize that, since the medium is thin, the conversion efficiency would be very small unless a substantial coherence is prepared.

Equation (1) shows that the statistical properties of the sidebands are determined by the properties of the probe and the prepared coherence. When the probe field is a statistically random quantity while the fluctuations in the driving fields and, consequently, in the prepared coherence are negligible, the probe field and the sidebands have the same normalized correlation functions, that is, the same statistical properties.

When solid hydrogen is used as a nonlinear medium, a sufficiently large Raman coherence can be easily prepared for the pure vibrational transition $Q_1(0)$ [5,7]. The states $|a\rangle$ and $|b\rangle$ are the ground ($v=0, J=0$) and pure vibrational ($v=1$, $J=0$) states, respectively, with the energy separation $\omega_{ba}=4149.64\,\mathrm{cm}^{-1}$, see Fig. 1(b). The medium is driven by two coaxial single-mode laser fields E_p and E_s, slightly detuned from the Raman resonance by a detuning δ. When the medium is adiabatically prepared in the phased or antiphased state, the Raman coherence is [4,8]

$$\rho_{ab} = \mathrm{sgn}(\delta)\,\frac{\Omega_{ab}}{\sqrt{(\delta+\Omega_{\mathrm{stark}})^2+4|\Omega_{ab}|^2}}. \tag{3}$$

Here $\Omega_{\mathrm{stark}} \cong (a_s-b_s)(|E_p|^2+|E_s|^2)/2$ is the Stark shift and $\Omega_{ab} \cong (d_s|E_sE_p|/2)e^{i(\phi_0-\kappa_c z)}$ with $\kappa_c=\beta_p a_p-\beta_s a_s$ is the two-photon Rabi frequency. The adiabatic preparation requires the condition $|\delta| \gg \delta\omega_L \gg \gamma_{ab}$, where γ_{ab} is the dephasing rate of the medium and $\delta\omega_L$ is the laser linewidth [4,8]. For the $Q_1(0)$ transition in solid hydrogen, the dephasing rate γ_{ab} is extremely low (<1.5 MHz [9]), even much lower than that in high-pressure hydrogen gas [10]. Therefore, the two-photon detuning δ can be set to a small value, allowing the generation of a sufficiently large coherence with relatively weak driving fields. We estimate the necessary intensity of the driving fields for the production of a substantial coherence to satisfy condition (2). Assuming the probe frequency $\omega_0=20\,000\,\mathrm{cm}^{-1}$ and using the parameters of hydrogen [11], we obtain $g \cong 3000\ \mathrm{cm}^{-1}$, $\Delta\kappa \cong 25\ \mathrm{cm}^{-1}$, and $\Delta\kappa_c \cong 130\,\mathrm{cm}^{-1}$. Hence, condition (2) requires $|\rho_{ab}| \gg 0.01$. We choose $\delta=-50$ MHz, take $|E_p|=|E_s|$, and use the parameters $(a_0,b_0,d_0)=(4.49,4.88,0.57)\times 10^{-7}$ in the SI units [8,11]. Then we find that a driving intensity of as low as 90 MW/cm^2 can produce a substantial coherence $|\rho_{ab}| \cong 0.05$. This coherence is large enough to satisfy condition (2) for efficient frequency conversion.

Now we proceed with the experimental part. A solid parahydrogen crystal was grown from the liquid phase in an optical cell with two sapphire windows [12]. The purity of parahydrogen obtained by converting normal liquid hydrogen with a catalyst at around 14 K was greater than 99.9%. The crystal was optically transparent without any visible cracks. We set the crystal thickness to 300 μm adjusting the separation between the windows. This thickness is shorter than the coherence length $l_{\mathrm{coh}} \cong 500\,\mu$m, and is enough for efficient conversion if a coherence $|\rho_{ab}| \gg 0.01$ is prepared.

For the coherence preparation, we used two single-frequency pulsed laser systems, a yttrium-aluminum-garnet (YAG) laser at 1064 nm (ω_s), and a Ti:sapphire laser at 738 nm (ω_p). Both systems were injection seeded by continuous-wave single-frequency lasers. The pulse durations [full width at half maximum (FWHM)] of the YAG and Ti:sapphire outputs were 12 and 24 ns, respectively. Their linewidths were 30 ± 4 and 15 ± 2 MHz, respectively, satisfying the Fourier-transform-limit condition. The laser beams were temporally superposed and coaxially focused into the crystal with diameter of 600 μm. We set the peak intensities of the driving fields to be the same. We chose the Raman detuning $\delta=-50$ MHz, at which the condition for the adiabatic coherence preparation was satisfied and a large value of $|\rho_{ab}|$ was achieved [8].

For the incoherent light, we used a fluorescent light from a dye solution (Coumarin-500) pumped by a weak YAG-laser output at 355 nm. The fluorescent light (pulse duration of 5.2 ns) had a broad, smooth continuous spectrum of 1770 cm^{-1} FWHM (493–540 nm). Its intensity distribution is uniform over the entire solid angle (4π sr). We picked up the fluorescent light partially in space and focused it with a lens onto a 50-μm-diameter pinhole, and then transferred the pinhole image to a 500-μm-diameter spot size at the crystal. The fluorescent light beam was parallel over a 1-mm-long spatial region including the crystal. We set the fluorescent light beam coaxial with the driving beams, and carefully adjusted the temporal and spatial overlaps between the beams in the 300-μm-long crystal. It should be noted here that the thin interaction length of 300-μm enables the beating of the coherence with even unfocusable lights such as incoherent lights.

We employed an optical multichannel analyzer to measure the forward emission spectra. To observe only the Raman sidebands of the fluorescent light, we blocked the driving beams and their Raman sidebands by a small spatial mask and notch filters. The relative sensitivity of the detection system for different frequencies was calibrated by a standard light source.

The measurements of the Raman sideband spectra were carried out for two cases, with different bandwidths of the

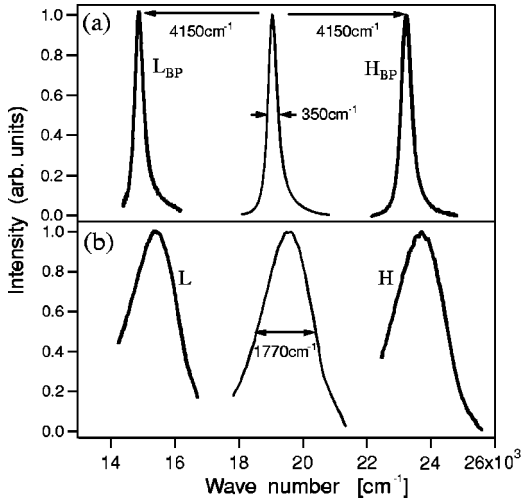

FIG. 2. Spectra of the sideband of the incident fluorescent light. (a) The bandwidth of the incident light is reduced to 350 cm^{-1} by using a bandpass filter. (b) The whole 1770-cm^{-1} bandwidth of the incident light is used. L_{BP} and L (H_{BP} and H) are the lower-frequency (higher-frequency) sidebands. The intensity in each spectrum is normalized to its peak value.

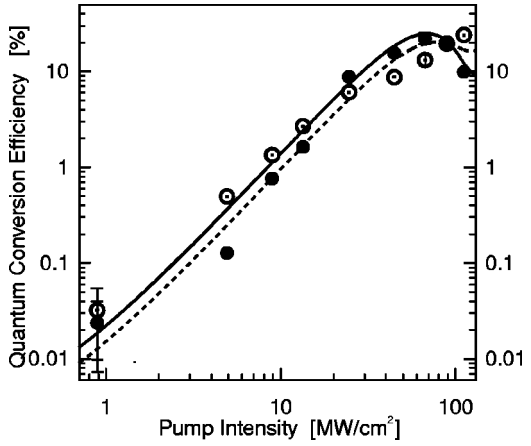

FIG. 3. Quantum conversion efficiency of the incident fluorescent light (1770 cm^{-1} FWHM) to its Raman sidebands as a function of the driving laser intensity. The observed data for the higher- and lower-frequency sidebands are shown by the solid and open circles, respectively. The calculated data are shown by the solid and dotted lines, respectively.

incident fluorescent light. First, we restricted the bandwidth of the incident fluorescent beam to 350 cm^{-1} FWHM by using a bandpass filter. The driving laser intensity was 110 MW/cm^2. Figure 2(a) shows the observed spectra of the sidebands including the incident fluorescent light. As seen, two continuous spectral profiles H_{BP} and L_{BP}, nearly identical to that of the incident beam, appear in the regions of wavelengths 409–441 nm and 620–696 nm, respectively. The frequency separation between the sidebands H_{BP} and L_{BP} is 4150 cm^{-1}, the same as the Raman shift. The two sidebands were observed collinearly on the axis of the incident beam, and had the same beam divergence as that of the incident beam. One understands that H_{BP} and L_{BP} are the Raman sidebands of the incident fluorescence and that the *incoherent* fluorescence light beats with the prepared Raman coherence without any restriction on the medium refractive index dispersion. Next, we removed the bandpass filter, and measured the spectra of the sidebands of the incident light with the whole 1770 cm^{-1} bandwidth, see Fig. 2(b). Again, the spectrum of the incident light was replicated very well at the Raman sidebands. Thus, the beating of the fluorescent light with the prepared Raman coherence replicated the incoherent nature into the Raman sidebands regardless of the spectral profile of the incident beam.

We measured the quantum conversion efficiency of the incident fluorescent light to the Raman sidebands for various driving laser intensities. The measurements were carried out for the cases with the incident beam bandwidths of 350 and 1770 cm^{-1}. The obtained results were essentially identical for the two cases. Figure 3 shows the results for the case with the bandwidth of 1770 cm^{-1}. The incident beam intensity was maintained at 1.5 kW/cm^2 corresponding to the pulse energy of 15 nJ. As seen from the figure, the conversion efficiency improves quadratically as the driving intensity increases until 30 MW/cm^2, and it almost saturates and even begins to decrease when the driving intensity is about 80 MW/cm^2. The conversion efficiency reaches the peak values 22% and 24% for the higher- and lower-frequency sidebands, respectively. The solid and dotted curves represent the results of the numerical simulations for the higher- and lower-frequency sidebands, respectively. The numerical simulations were based on the wave propagation equations for the three coupled fields with the prepared coherence $\rho_{ab}(z) = |\rho_{ab}(0)|e^{-\kappa_c z}$ as a fitting parameter. The effective spatial overlap between the probe and driving beams was taken into account. As seen, the calculations reproduce very well the characteristic behavior of the observed data. The decrease of the conversion efficiency after saturation indicates that the term sz in Eqs. (1) has exceeded $\pi/2$. Through the simulations and the fitting, the largest Raman coherence generated at the driving intensity of 110 MW/cm^2 is estimated to be $|\rho_{ab}| \cong 0.04$. Due to this coherence, substantial frequency conversion within a coherence length has been realized.

Unlike the case of Fig. 3, we now fix the driving intensity and, consequently, the prepared Raman coherence, but vary the incident fluorescent light intensity. According to Eqs. (1), the conversion efficiency of the probe field to its sidebands does not depend on the probe intensity. Figure 4 shows the observed quantum conversion efficiency for the higher-frequency sideband as a function of the incident fluorescence intensity (bottom axis). The driving intensity was fixed at 70 MW/cm^2. We used low probe intensities varying from 32 to 1000 W/cm^2. The figure shows that the conversion efficiency remains constant and high (at 22%) within the experimental errors, even when the probe intensity is reduced to 32 W/cm^2 corresponding to the incident energy of 330 pJ.

Since the probe light used in our experiments was temporally and spatially incoherent, we estimate the photon number per coherent wave packet in both time and space regions. The number of coherent wave packets in time domain is defined as the ratio of the pulse duration (5.2 ns) to the autocorrelation (coherence) time (12 fs), which is derived

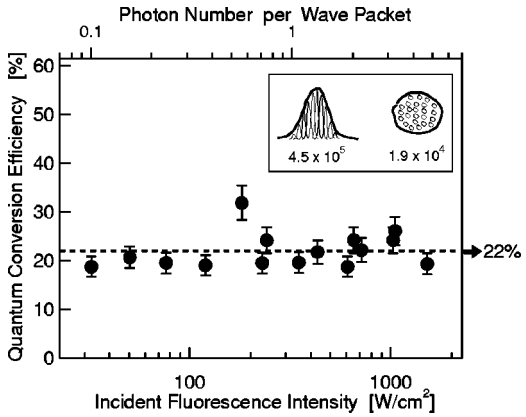

FIG. 4. Quantum conversion efficiency of the incident fluorescent light (1770 cm^{-1} FWHM) to its higher-frequency Raman sideband as a function of the incident intensity (bottom axis) or the incident photon number per wave packet (top axis). The inset shows the wave-packet number in time (4.5×10^5) and that in space (1.9×10^4).

from the Fourier transformation of the fluorescence spectrum (1770 cm^{-1} FWHM). This number is evaluated to be 4.5×10^5. The number of coherent wave packets in space domain is defined as the ratio of the focus area (0.25 mm^2) of the fluorescent light to that (13 μm^2) of a single-transverse-mode laser beam with similar wavelength and spatial beam profile. This number is estimated to be 1.9×10^4. Therefore, the total number of coherent wave packets, defined as the product of the numbers of wave packets in time and space, is 8.6×10^9. When the incident fluorescent beam intensity is 300 W/cm^2 (3.3 nJ), the total photon number of the beam amounts to $\sim8.6\times10^9$, corresponding to one photon per wave packet. The new scale using photon number per coherent wave packet is shown as the top axis in Fig. 3. This scale shows that the quantum conversion efficiency is maintained constant and high, at 22%, even for weak fluorescent lights with less than one photon per wave packet.

In conclusion, we have shown that a sufficiently large Raman coherence prepared in a thin hydrogen crystal, acting like a local oscillator at a frequency of 4150 cm^{-1}, modulates an incoherent fluorescent light and replicates efficiently the 1770-cm^{-1} huge bandwidth of the light into the Raman sidebands. Since the bandwidth of 1770 cm^{-1} corresponds to an autocorrelation time of 12 fs, our technique can naturally be extended to replicate a femtosecond pulse into the 4150-cm^{-1} higher- and lower-frequency sidebands, whose Fourier synthesis may result in single sub-fs pulses.

The authors thank M. Suzuki for his contribution in low-temperature experiments. One of the authors (M.K.) thanks H. Yoneda for helpful discussions.

[1] Y. R. Shen, *The Principles of Nonlinear Optics* (Wiley, New York, 1984).
[2] P. Di Trapani, A. Andreoni, P. Foggi, C. Solcia, R. Danielius, and A. Piskarskas, Opt. Commun. **119**, 327 (1995).
[3] J. Shan, IEEE J. Quantum Electron. **24**, 276 (1988).
[4] S. E. Harris and A. V. Sokolov, Phys. Rev. A **55**, R4019 (1997); Phys. Rev. Lett. **81**, 2894 (1998).
[5] K. Hakuta, M. Suzuki, M. Katsuragawa, and J. Z. Li, Phys. Rev. Lett. **79**, 209 (1997).
[6] A. V. Sokolov, D. R. Walker, D. D. Yavuz, G. Y. Yin, and S. E. Harris, Phys. Rev. Lett. **85**, 562 (2000).
[7] J. Q. Liang, M. Katsuragawa, Fam Le Kien, and K. Hakuta, Phys. Rev. Lett. **85**, 2474 (2000).
[8] Fam Le Kien, J. Q. Liang, M. Katsuragawa, K. Ohtsuki, K. Hakuta, and A. V. Sokolov, Phys. Rev. A **60**, 1562 (1999).
[9] J. Z. Li, M. Katsuragawa, M. Suzuki, and K. Hakuta, Phys. Rev. A **58**, R58 (1998).
[10] W. K. Bischel and M. J. Dyer, Phys. Rev. A **33**, 3113 (1986); J. J. Ottusch and D. A. Rockwell, IEEE J. Quantum Electron. **24**, 2080 (1988).
[11] P. C. Souers, *Hydrogen Properties for Fusion Energy* (University of California, Berkeley, 1986); A. C. Allison and A. Dalgarno, At. Data **1**, 289 (1970).
[12] M. Suzuki, M. Katsuragawa, R. S. D. Sihombing, J. Z. Li, and K. Hakuta, J. Low Temp. Phys. **111**, 463 (1998).